

## Stalling of near-inertial waves in a cyclone

L.-Y. Oey,<sup>1</sup> M. Inoue,<sup>2,3</sup> R. Lai,<sup>4</sup> X.-H. Lin,<sup>1</sup> S. E. Welsh,<sup>3</sup> and L. J. Rouse Jr.<sup>2,3</sup>

Received 8 April 2008; accepted 2 May 2008; published 20 June 2008.

[1] Observations at the edge of the Loop Current after hurricane Katrina show inertial energy amplified at a depth of approximately 600~700 m. Ray-analysis using the eddy field obtained from a numerical simulation with data assimilation suggests that the amplification is due to inertial motions stalled in a deep cyclone. **Citation:** Oey, L.-Y., M. Inoue, R. Lai, X.-H. Lin, S. E. Welsh, and L. J. Rouse Jr. (2008), Stalling of near-inertial waves in a cyclone, *Geophys. Res. Lett.*, 35, L12604, doi:10.1029/2008GL034273.

### 1. Introduction

[2] Near-inertial waves generally have frequencies above  $f_{eff} = f(1 + \zeta/f)^{1/2} \approx f + \zeta/2$  for small Rossby number =  $\zeta/f$  in (background) flow with non-zero vorticity  $\zeta$  [Mooers, 1975; Kunze, 1985, hereinafter referred to as K85]. Inertial energy initiated in a region with more negative vorticity than its surroundings would then tend to be trapped, for example, inside an anticyclonic vortex, resulting in vertical “chimneying” of near-inertial waves to subsurface [Zhai *et al.*, 2007]. Shay *et al.* [1998] observed strong inertial motions ( $0.06 \text{ m s}^{-1}$ ) at a 725 m depth in a warm ring in the western Gulf of Mexico after the passage of hurricane Gilbert. Kunze [1985] explains that, in the case of a baroclinic eddy (e.g., warm rings, or the Loop Current), there can be vertical trapping and mixing in a critical layer (see Kunze *et al.* [1995] for turbulence measurements in a Gulf Stream warm ring and for an excellent review with other references).

[3] By the same reasoning, once generated near the surface, near-inertial waves tend to radiate away over a cyclone (defined as a localized region where  $\zeta > 0$ ); “chimneys” and trapping are less likely. However, background flow and topography of  $f_{eff}$  can be quite complex. Thus, near-inertial waves may enter a subsurface mesoscale field and be surrounded by strong positive vorticity beneath and to one side, i.e., in a frontal cyclone, where inertial motions may then stall. Here, we describe such a stalling at a mooring (see location in Figure 1) near the Loop Current in the Gulf of Mexico after the passage of hurricane Katrina. Huang *et al.*'s [1998; see also Lai and Huang, 2005] Empirical Mode Decomposition is used to extract the near-inertial wave amplitude and frequency modulations.

A numerical model is used to estimate the eddy field which is then used to calculate energy paths by ray-tracing.

### 2. Data

[4] The LSU (Louisiana State University) mooring consists of two ADCPs, one upward-looking set at 140 m and the other downward-looking set at 3200 m at ( $87^\circ\text{W}$ ,  $25.5^\circ\text{N}$ ; Figure 1) in water of 3356 m where the bottom is relatively flat. Additional Aanderra current meters were deployed between the two ADCPs to sample the entire water column. The top ADCP measured near-surface currents up to  $z = -60$  m, while the bottom ADCP sampled near-bottom currents; the bottom-most currents were measured at  $z = -3340$  m. The period was May/30–Nov/30/2005. This paper focuses on near-inertial waves produced by hurricane Katrina (Aug/26–30/2005), when the mooring was located near the northwestern edge of the Loop Current. We focus on the upper-level currents, roughly from  $z \approx -100$  m to about  $-1500$  m below. Data return was excellent. The data is averaged and sampled hourly. More details are given by Inoue *et al.* [2008].

### 3. Models

[5] The Princeton Ocean Model [henceforth “the model;” <http://www.aos.princeton.edu/WWWPUBLIC/htdocs.pom/>] is used to provide the background flow for ray-tracing (below). The model includes Loop Current and rings, assimilated using satellite data up to 7 days prior to a hurricane’s entrance into the Gulf of Mexico; thereafter the model is run for 16 days without further assimilation. The model has been extensively checked against observations [e.g., Yin and Oey, 2007] (see also <http://www.aos.princeton.edu/WWWPUBLIC/PROFS/publications.html>). The model horizontal grid  $\Delta$  is variable from 3 km (northern slope) to 10 km (near the Yucatan Channel). For this work, 51 (instead of 26 in previous work) terrain-following sigma levels are used in the vertical, with approximately 23 in the upper 1500 m of the water column.

[6] The numerical model’s resolution is too coarse particularly in the vertical in which  $\Delta z \approx O(2\pi/k_3) \approx O(100 \text{ m})$ , where  $k_3$  = vertical component of the wavevector  $\mathbf{k}$ . Thus, the model can only describe qualitatively the structures of the near-inertial wave field, and we take it more as providing the slow background field through which near-inertial waves propagate.

[7] The ray equations [K85] have reduced physics but these can be computed very accurately to describe near-inertial wave propagation. The theory assumes small Rossby number and large geostrophic Richardson number  $Ri$ , but includes their effects (to first order) through  $f_{eff}$  and

<sup>1</sup>Program in Atmospheric and Oceanic Sciences, Princeton University, Princeton, New Jersey, USA.

<sup>2</sup>Department of Oceanography and Coastal Sciences, Louisiana State University, Baton Rouge, Louisiana, USA.

<sup>3</sup>Coastal Studies Institute, Louisiana State University, Baton Rouge, Louisiana, USA.

<sup>4</sup>Minerals Management Service, Herndon, Virginia, USA.

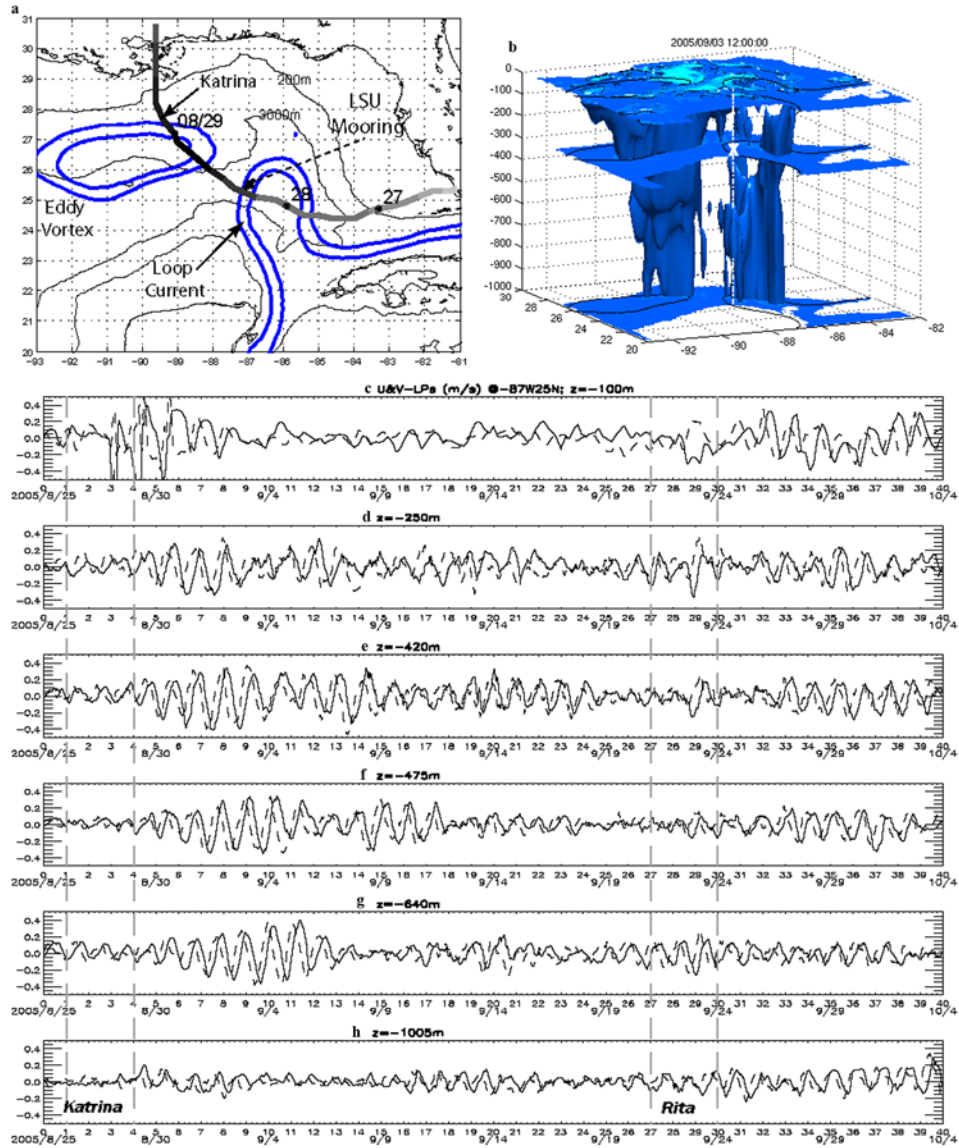


**Figure 1.** (a) Study area showing mooring location, Katrina track (dark indicates wind speed  $>60$  m/s), and the thick contours are SSH = 0, 0.2 m. (b) The 3-d surface of inertial energy =  $0.03 \text{ m}^2 \text{ s}^{-2}$  on Sep/03/12:00. (c)–(h) Observed high-passed  $u$  (west-east; solid) and  $v$  (dashed) velocities (m/s) at the mooring at the indicated depths, during hurricanes Katrina (Aug/26~29) and Rita (Sep/21~24).

vertical (geostrophic) shears  $\partial \mathbf{u}_h / \partial z$  ( $\mathbf{u}_h = (u, v)$ , horizontal velocity). The Eulerian frequency

$$\omega \approx f_{\text{eff}} + N^2 k_h^2 / (2f k_3^2) + (\partial \mathbf{u} / \partial z \times \mathbf{k}) \cdot \mathbf{n}_3 / k_3 + \mathbf{k} \cdot \mathbf{u} \quad (1)$$

is the sum of the intrinsic ( $\omega_0$ ) and Doppler-shift ( $\mathbf{k} \cdot \mathbf{u}$ ) frequencies, and is constant along the ray. Here,  $\mathbf{u} = (u, v, w)$ ,  $N^2 =$  squared buoyancy frequency,  $k_h^2 = k_1^2 + k_2^2$  is the squared horizontal wavenumber and  $\mathbf{n}_3$  is the unit vector in  $z$ . The ray equations

$$dx_i / dt = \partial \omega / \partial k_i + u_i \quad (2a)$$

$$dk_i / dt = -\partial \omega / \partial x_i, \quad (2b)$$

where  $i = 1, 2$  and  $3$ ,  $x_i$  is the position vector, are solved using the fourth-order Runge-Kutta scheme with a time step = 0.1 hour. The modeled  $(u, v)$  field is used to estimate the (initial) horizontal wavelengths using a method by Mied *et al.* [1986]; this yields a range of estimates of  $2\pi/k_h = 35 \sim 70$  km. Similarly, the observed  $(u, v)$  at the mooring yield estimates of vertical wavelengths  $2\pi/k_z = 70 \sim 140$  m. Thousands of rays were initiated with these ranges of vertical and horizontal wavelengths as well as all possible horizontal wave propagation angles. The  $\mathbf{u}$ ,  $\zeta$ ,  $N^2$  and  $\partial \mathbf{u}_h / \partial z$  are 5-day averages following the storm from the model in accord with the slowly-varying background assumption of the ray equations.

#### 4. Results

[8] Figure 1a shows sea-surface height (SSH) contours showing the Loop Current and a newly-shed warm ring.

Figure 1b shows the three-dimensional surface of inertial energy  $((u^2 + v^2)/2 = 0.03 \text{ m}^2 \text{ s}^{-2})$  from the model, 6 days after Katrina (Sep/03/12:00) [cf. Wang and Oey, 2008]. Energetic inertial chimneys (amplitude  $\approx 0.24 \text{ m/s}$ ) penetrate to 1000-m depth to the right of the storm in the Loop Current and warm-core ring. As seen in animation (not shown) and ray-tracing (below), the chimneys are advected anticyclonically around the rims of the Loop Current and warm ring. Under the Loop Current, penetration is deeper on the eastern side ( $>1200 \text{ m}$  compared to  $800 \text{ m}$  in the west). Regions outside the Loop Current and warm ring are void of these strong inertial chimneys. The region of low SSH or cyclonic vorticity between the Loop Current and the warm ring will be shown to be where super-inertial waves are produced by the storm.

[9] Katrina winds  $(|u_a| > 60 \text{ m/s})$  produced a strong near-inertial response at the mooring. This consists of clockwise-rotating currents that propagate downward (Figure 1c–g; hurricane Rita is included for comparison). In the case of Katrina, the response penetrates and amplifies to depths of about  $z = -640 \text{ m}$  with amplitudes exceeding  $0.3 \text{ m/s}$  around Sep/05. The amplitude attenuates at  $z = -760 \text{ m}$  (not shown) to approximately  $0.15 \text{ m/s}$ , and quite abruptly drops to  $\approx 0.1 \text{ m/s}$  at  $z = -1005 \text{ m}$  (Figure 1h). The response to Rita is less both in terms of amplitudes and depths of penetration.

#### 4.1. Empirical Mode Decomposition Analysis

[10] We use Empirical Mode Decomposition to extract various Intrinsic Mode Functions then compute their Hilbert spectra [Huang et al., 1998]. Unlike FFT, Huang et al.'s method can accommodate rapid frequency variations with little spurious harmonics. The time series can be non-stationary as well as non-linear. The method is efficient; for our time series, it yields only nine intrinsic modes each of which (after the Hilbert transform) gives frequency and amplitude as a function of time. The first mode is of O(hours) period and of very small amplitude, while the ninth is the 'residue' which is (nearly) constant (in time) and also has very small amplitude ( $\text{rms} \sim 10^{-4} \text{ m/s}$ ).

[11] The second and third modes have near-inertial periods. Their Hilbert spectra for the 6-month period Jun–Nov/2005 near the surface ( $z \approx -250 \text{ m}$ ; not shown) indicate strong near-inertial variability both in amplitude and frequency, and a tendency for sub- (super-)inertial waves to be produced when the mooring is inside (outside) the Loop Current where vorticity  $\zeta < 0$  ( $\zeta > 0$ ). Figure 2a shows spectra at  $z = -640 \text{ m}$ , focusing on the response to Katrina. After the storm, energetic super-inertial ( $\omega/f > 1$ ) signals arrive at the mooring before sub-inertial (Figure 2a). The distribution of energy is skewed to  $\omega/f < 1$  in the upper 1000 m (Figure 2b) because during the 6-month observation the mooring was located predominantly within the negative-vorticity part of the Loop Current. Near-inertial energy is intensified subsurface near 500–700 m depth.

#### 4.2. Ray Analysis

[12] The Loop Current and warm ring play an important role in horizontally advecting and confining near-inertial waves into "chimneys" (Figure 1). Experiments with initially-level isopycnals (i.e., no Loop Current and rings; not shown) produce near-inertial response confined to the upper

200 m. We now use the model flow field and show by way of ray-tracing how the subsurface intensification (Figure 2b) may be explained by stalling, i.e., vanishing of  $\mathbf{u} + \mathbf{C}_g$ , where  $\mathbf{C}_g = (C_{g1}, C_{g2}, C_{g3})$  is the group velocity, along rays at the base of the Loop Current.

[13] Each ray is traced from the mooring at  $z = -600 \text{ m}$ , with initial vertical wavelengths  $2\pi/k_z$  incrementally looped from 70–140 m, horizontal wavelengths  $2\pi/k_h$  from 35–70 km and wave-angles  $\tan^{-1}(k_2/k_1)$  from  $-\pi$  through  $\pi$ . Rays are excluded if they do not pass above  $z = -200 \text{ m}$  or if they do, no portion of the ray comes within 100 km on either side of Katrina. These limits are reasonable for inertial energy originating from the storm, and result in two (more manageable) groups of rays represented by Rays#1W and 1E respectively in Figure 2c. Ray#1W (1E) represents super- (sub-) inertial waves originating from the west (east) or cyclonic (anticyclonic) side of the Loop Current in the proximity of the storm's track. Other rays that do not pass through the mooring at  $z \approx -600 \text{ m}$  are also similarly traced using the same ranges of wavelengths and wave-angles, as well as the same "exclusion" criterion; examples are rays 2, 3 and 4 in Figure 2c.

[14] Ray#1W shows that the near-inertial wave energy observed at  $z \approx -600 \text{ m}$  (Figure 2b) originates near the surface ( $z = -100 \text{ m}$ ) approximately 70 km west and 20 km north of the mooring, i.e., near the Katrina's center on Aug/28/10:00GMT between the Loop Current and warm ring, in a region of positive  $\zeta$  so that  $f_{eff} > f$ . The ray propagates towards the base of the Loop Current ( $z \approx -600 \text{ m}$  of the mooring); the arrival time, 4–6 days later, approximately agrees with that observed (Figure 1). The ray 'stalls' near  $z = -600 \text{ m}$  (crowding of the daily markers '\*'), for about 7 days), suggesting an accumulation of energy there. This coincides with the observed intensification of energy near this depth (Figure 2b). We explain the cause of this stalling below.

[15] Loop Current frontal cyclones are often seen in high-resolution satellite SST [e.g., <http://fermi.jhuapl.edu/avhrr/gm/averages/index.html>]. These cyclones originate as small perturbations along the highly sheared current on the western side of the Loop Current in the Yucatan Channel and amplify (in the model) through baroclinic instability over the north Campeche Bank as the Loop Current enters the deep water of the Gulf of Mexico; the LSU mooring is located where frontal cyclones often pass [Oey, 2008]. During Katrina, the model suggests that a subsurface cyclonic meander sat astride the mooring. Figure 3a shows this with  $\zeta/f$  (color) and velocity at  $z = -600 \text{ m}$  where a subsurface cyclone with maximum  $\zeta/f \approx +0.4$  and a diameter of about 70–100 km is seen. From the surface, where  $\zeta/f \approx +0.23$ , ray#1W first propagates downward (towards the Loop Current) through an environment of weaker and slightly negative  $\zeta$  before encountering the cyclone where  $f_{eff}$  increases under and east of the ray. The ray's intrinsic frequency tends to  $f_{eff}$  as  $(k_h/k_3)^2$  (see equation 1) and the group velocity (see K85's equation 11) become small near the cyclone. There is also upwelling,  $u_3 \approx +30 \text{ m/day}$  (not shown), which counters the downward  $C_{g3}$  and helps to maintain the vertical stalling.

[16] The role of strong positive  $\zeta$  and its gradients on stalling may be made more precise by examining how  $k_h^2$

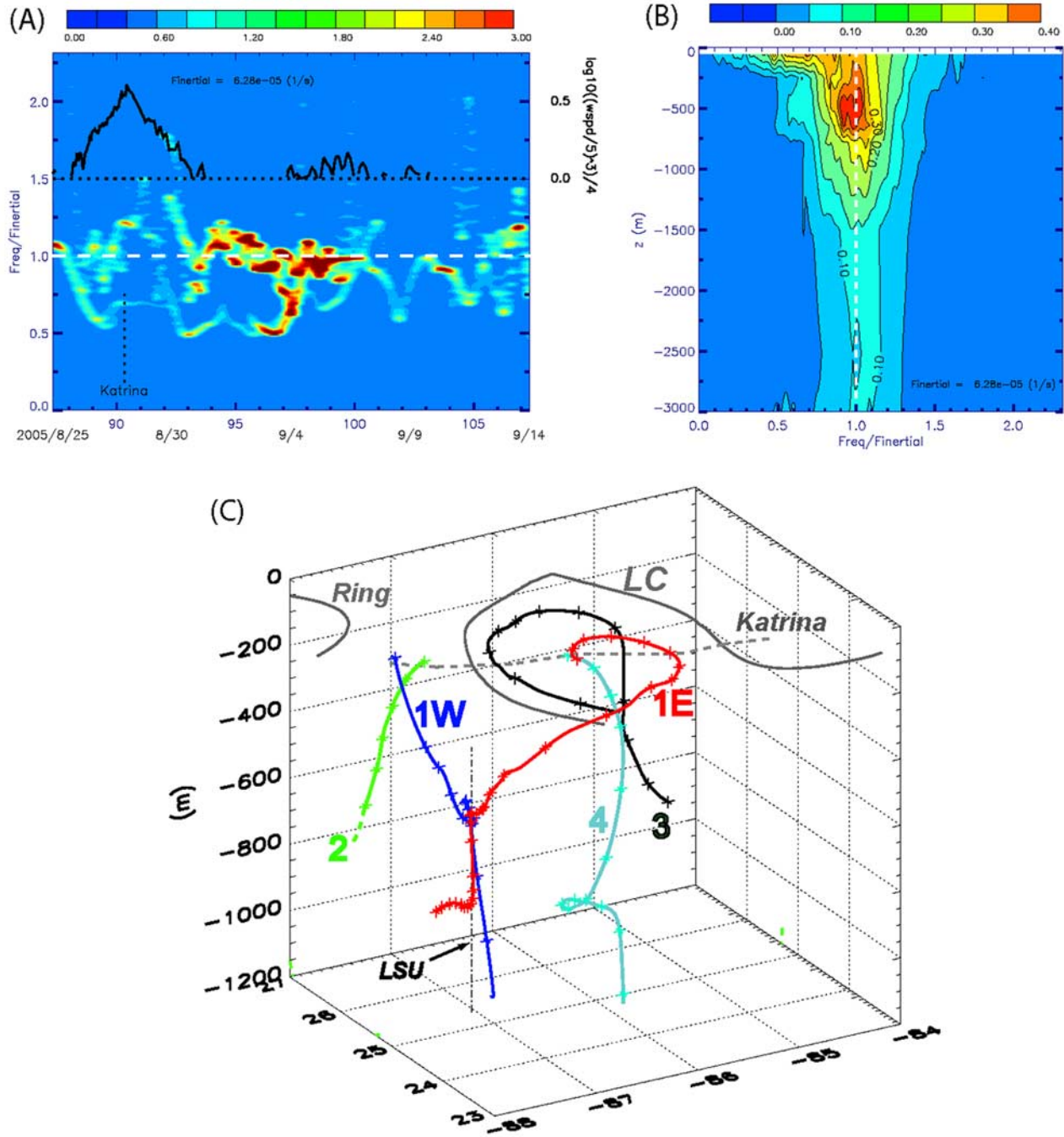


**Figure 2.** (a) Hilbert energy spectra (color; unit:  $10^{-2} \text{ m}^2 \text{ s}^{-2}$ ) of near-inertial currents at  $z = -640$  m as a function of time (days since May/30/2005 and date are shown) and  $\omega/f$ . Black line is the wind power  $P_w = \log_{10}[(|u_a|/5)^3]/4$  (plot positive only) at NDBC 42003 ( $25.74^\circ\text{N}$ ,  $85.73^\circ\text{W}$ ) near the LSU mooring. (b) Time-averaged (over 6-month) Hilbert spectra as a function of  $\omega/f$  and depth. (c) near-inertial wave rays “1” through “4” marked daily (by asterisks). The Loop Current, ring and Katrina track are shown.

and  $k_3^2$  behave along the ray near the cyclone. Taking the dot product of  $\mathbf{k}$  with equation (2b), and using (1):

$$d(k_h^2)/dt \approx -\mathbf{k}_h \cdot \nabla \zeta + (k_h^2/k_3)(\partial \zeta / \partial z) \quad (3a)$$

$$d(k_3^2)/dt \approx -k_3[(\partial \zeta / \partial z) + k_h^2/(fk_z^2) \partial N^2 / \partial z + 2(\mathbf{k}_h \times \nabla B)_z / f] \quad (3b)$$

Here, several small terms involving  $\nabla N^2$ ,  $w$ ,  $u_{zz}$  and  $v_{zz}$  are dropped, and  $B = g\rho/\rho_0$ . Approaching the subsurface cyclone from northwest and surface, we have  $(k_1, k_2, k_3) = (>0, <0, >0)$ ; the vector  $(k_1, k_2)$  makes an angle a little less than  $45^\circ$  clockwise from the  $x$ -axis so that, since  $\nabla \zeta$  points eastward towards the cyclone, we have  $\mathbf{k}_h \nabla \zeta > 0$ . Also,  $\partial \zeta / \partial z < 0$  and therefore  $k_h^2$  tends to zero from (3a). This is confirmed by plots (not shown) which show that  $k_h$

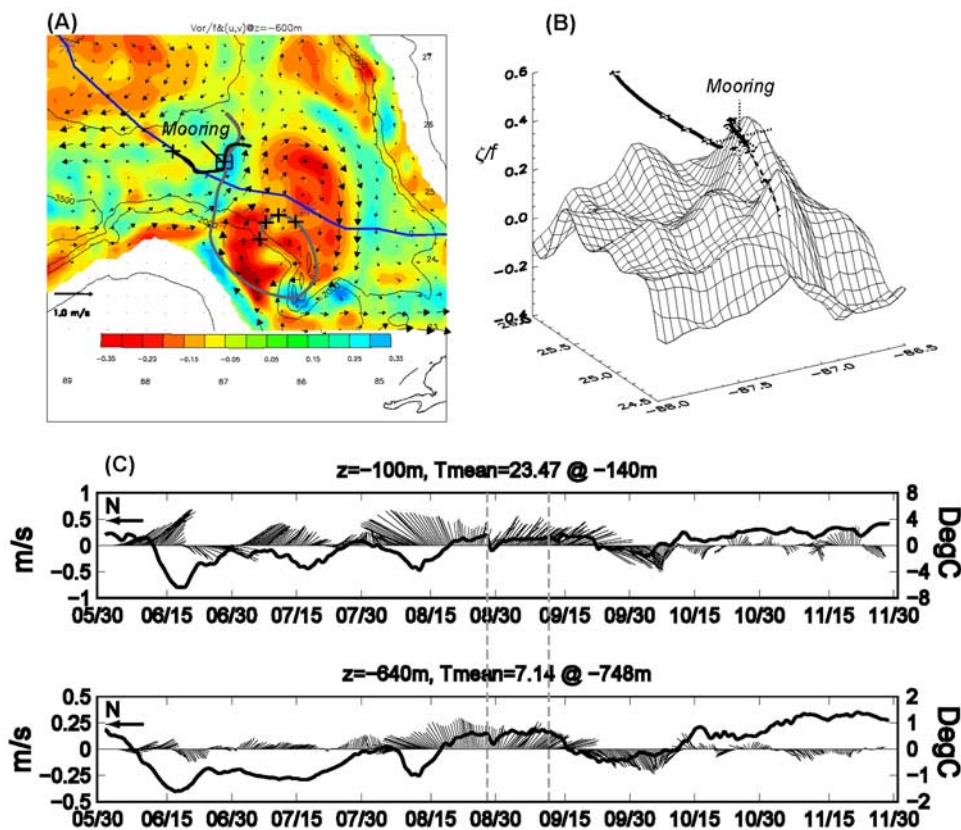


**Figure 3.** (a) Modeled vectors (shown every 4 grid points) and  $\zeta/f$  (colors) at  $z = -600$  m. The mooring location is where super-(black) and sub-(dark grey) inertial rays pass at  $z = -600$  m; shown are rays projected onto the  $xy$ -plane. The rays' locations at  $z = -100$  m are marked by pluses which also mark the first 3-daily locations of the sub-inertial ray. Katrina track is shown in blue and the two asterisks on it mark the storm's positions on Aug/28 and Aug/29, respectively. (b) The same  $\zeta/f$  plotted as 3-d surface toward which ray#1W propagates. (c) Observed 40-hour low-passed velocity shown as sticks at  $z = -100$  m and  $z = -640$  m with positive  $y$ -axis pointing due east, and temperature time-series (solid line) shown as deviation from the mean shown at the indicated depths. The temperatures are taken from the depths nearest to the depths of the ADCP velocity measurements. Period when near-inertial waves are prevalent is bracketed in grey dashed lines.

decreases and  $k_3$  increases near the cyclone. From (3b), the last two terms  $\partial N^2/\partial z$  and  $(\mathbf{k}_h \times \nabla B)|_z/f$  are both positive ( $\nabla B$  points eastward towards the cyclone's center) so they cannot account for the increase in  $k_3$  and  $\partial \zeta/\partial z < 0$  is principally responsible for the increase in  $k_3$ .

[17] Wang [1991] (based on Mooers [1975]) found that anomalously-low-frequency ( $\omega < f_{eff}$ ) waves from the cold side of a front can be trapped vertically subsurface where isopycnals become flat [see [http://www.aos.princeton.edu/WWWPUBLIC/PROFS/PUBLICATION/oeysel\\_footnote\\_on\\_alf\\_waves.pdf](http://www.aos.princeton.edu/WWWPUBLIC/PROFS/PUBLICATION/oeysel_footnote_on_alf_waves.pdf)]. We find that some rays (about 10%) are anomalously-low-frequency. However, vertical trapping alone cannot explain why a ray stalls. Figure 3a shows that the ray at  $z \approx -600$  m comes very near the center of the cyclone (defined as the location where  $\zeta/f$  is a maximum  $\approx +0.4$ ), but does not cross it. This behavior is seen in Figure 3b which displays the  $\zeta/f$  as a surface towards which the ray propagates from above. In addition to being blocked from below, the ray bends northward being blocked also by the  $\zeta/f$ -ridge formed by the strong cyclonic meander, consistent with the above discussion on equation (3). Since  $k_h^2$  and  $k_3^2$

are nonnegative, (3) puts a strong constraint on the allowable space to which ray paths may traverse. As seen in Figures 2c, 3a, and 3b, the Ray1W cannot penetrate below the cyclone, nor to the east of the cyclone where the strong positive  $\zeta$ -ridge is present. Thus, near-inertial motions are stalled inside the cyclone for a relatively long period of about 7 days before radiating horizontally and rapidly downward away from the mooring (Figure 2c).

[18] A similar "stalling" occurs for ray#1E (Figure 2c). However, after radiating away from the cyclonic ridge, since this ray is sub-inertial, it stalls a second time at  $z \approx -950$  m. Ray#1E is also strongly influenced by the Loop Current. It follows and remains in the near-surface anticyclone of the Loop Current for a relatively long time (5~6 days) before propagating downward towards the mooring at  $z = -600$  m. Though not shown here, other rays (by varying the initial wavenumbers; see above) originating on the western or cold (eastern or warm) side of the Loop Current behave similarly as ray#1W (1E). Similar results are also obtained for rays through  $z = -650$  m (instead of  $-600$  m); but rays below approximately  $z = -650$  m are

very different as they do not originate from the surface. In summary, observed intensification near  $z = -640$  m at the LSU mooring may be explained by an accumulation of energy caused by stalling of near-inertial waves by a subsurface cyclone, whose high  $f_{\text{eff}}/f > 1$  prevents energetic near-inertial motions from reaching greater depths. In the vertical, the cyclone acts like a near-inertial “umbrella” with its top at  $z \approx -600$  m to  $-650$  m. This explains why observed near-inertial amplitudes are weaker for  $z < \approx -1000$  m. The arrival at the mooring of energetic super-inertial waves before sub-inertial (Figure 2a) is due to the strong influence of the Loop Current on the latter waves as they are forced to loop around the anticyclone before escaping to deeper levels.

[19] Other rays in Figure 2c illustrate different aspects of near-inertial spreading. Ray#2 begins near the surface between the Loop Current and warm ring. It propagates into the “chimney” in the ring (where  $f_{\text{eff}}$  is reduced; Figure 1). Ray#3 begins at the western side of the Loop Current but within it, and displays a round-the-Loop Current progression as it is being advected anticyclonically to the eastern side, in rough agreement with the numerical simulation (Figure 1). There is no stalling in these two cases. Finally, ray#4 begins inside the Loop Current in a region of strongly negative  $\zeta/f (\approx -0.4$  at  $z = -100$  m). This ray stalls at  $z \approx -900$  m where  $\zeta/f$  reaches a local maximum ( $\approx -0.1$ ) and the ray’s intrinsic frequency  $\approx f_{\text{eff}} \approx 0.94 f$ . However, the modeled  $\zeta/f$  is complicated and  $\zeta/f$  decreases (more negative, not shown) below  $z \approx -900$  m. The combination of this and a strong downwelling velocity field,  $w \approx -50$  m/day, allows ray#4 to penetrate deeper.

## 5. Discussion and Conclusions

[20] The model cyclone spun up through an instability process [Oey, 2008]. There is indirect evidence that a cyclone was present. Firstly, the warm ring had separated or was in the process of separating from the Loop Current during Katrina (Figure 1), and shedding is often accompanied by the development of deep cyclones [e.g., Oey, 2008]. Secondly, observed temperature decreases and then rises before and after the storm (Figure 3c), a characteristic that is consistent with the passage of a cyclone. The velocity sticks suggest that the cyclone propagates approximately northeastward with the mooring to the right.

[21] Summarizing, measurements after hurricane Katrina indicate energetic near-inertial waves intensified at  $z \approx -640$  m, with amplitudes  $\approx 0.3$  m s<sup>-1</sup>. The first waves to arrive at the mooring are super-inertial and originate to the west and north of the Loop Current. Sub-inertial waves originate from near the Loop Current’s center, and spiral anticyclonically and downward following the Loop Current, arriving 1–2 days later. Both types of waves stall at  $z \approx -640$  m. Stalling is explained by waves entering a region where an intense subsurface frontal cyclone ( $\zeta/f \approx +0.4$ ) sat astride the mooring. As pointed out by one reviewer, the  $k_h$  and  $k_3$  plots (not shown) indicate that near the cyclone the former decreases faster than the former increases ( $k_3 \sim \infty$  would suggest a critical layer). In the present case, wave slows horizontally (though does not reflect: both  $k_1$  and  $k_2$

remain of one sign) resembling a turning-point behavior near the deep cyclone. The largest variation occurs in  $x$ , so that  $\omega \approx \omega(k_i, x)$ , and a ray-tube analysis [Lighthill, 1978] then suggests an energy-increase  $\sim k_1^{-1}$ , approximately a factor of 2 for ray#1W (or 1E).

[22] Stalling and trapping of near-inertial waves can lead to mixing [Lueck and Osborn, 1986; Kunze et al., 1995]. In the Gulf of Mexico, subsurface cyclones are ubiquitous features of deep-ocean eddy field [e.g., Oey, 2008]. Thus, in addition to anticyclones, the proposed mechanism of wave-stalling in subsurface cyclones can potentially contribute to deep mixing.

[23] **Acknowledgments.** We are grateful to the Minerals Management Service (MMS) for supports (Contract 1435-01-06-CT-39731 and 14-35-01-04-CA-32806). Encouragements from the program managers Carole Current and Alexis Lugo-Fernandez are appreciated. Comments from reviewers improve the manuscript. Computing was conducted at GFDL/NOAA.

## References

- Huang, N. E., et al. (1998), The empirical mode decomposition and the Hilbert spectrum for nonlinear and non-stationary time series analysis, *Proc. R. Soc. London, Ser. A*, 903–995.
- Inoue, M., S. E. Welsh, L. J. Rouse Jr., and E. Weeks (2008), Deepwater currents in the eastern Gulf of Mexico: Observations at 25.5°N and 87°W, *OCS Stud. MMS 2008-001*, 95 pp., U.S. Dep. of the Inter., New Orleans, La.
- Kunze, E. (1985), Near-inertial wave propagation in geostrophic shear, *J. Phys. Oceanogr.*, 15, 544–565.
- Kunze, E., R. W. Schmitt, and J. M. Toole (1995), The energy balance in a warm-core ring’s near-inertial critical layer, *J. Phys. Oceanogr.*, 25, 942–957.
- Lai, R. J., and N. Huang (2005), Investigation of vertical and horizontal momentum transfer in the Gulf of Mexico using empirical mode decomposition method, *J. Phys. Oceanogr.*, 35, 1383–1402.
- Lighthill, J. (1978), *Waves in Fluids*, 504 pp., Cambridge Univ. Press, Cambridge, U. K.
- Lueck, R., and T. Osborn (1986), The dissipation of kinetic energy in a warm-core ring, *J. Geophys. Res.*, 91, 803–818.
- Mied, R. P., C. Y. Shen, C. L. Trump, and G. L. Lindemann (1986), Internal-inertial waves in a Sargasso Sea front, *J. Phys. Oceanogr.*, 16, 1751–1762.
- Mooers, C. N. K. (1975), Several effects of a baroclinic current on the cross-stream propagation of inertial-internal waves, *Geophys. Fluid Dyn.*, 6, 245–275.
- Oey, L.-Y. (2008), Loop Current and deep eddies, *J. Phys. Oceanogr.*, in press.
- Shay, L. K., A. J. Mariano, S. D. Jacob, and E. H. Ryan (1998), Mean and near-inertial ocean current response to Hurricane Gilbert, *J. Phys. Oceanogr.*, 28, 858–889.
- Wang, D.-P. (1991), Generation and propagation of inertial waves in the subtropical front, *J. Mar. Res.*, 49, 619–633.
- Wang, D.-P., and L.-Y. Oey (2008), Hindcast of waves and currents in Hurricane Katrina, *Bull. Am. Meteorol. Soc.*, 89, 487–495.
- Yin, X.-Q., and L.-Y. Oey (2007), Bred-ensemble ocean forecast of Loop Current and rings, *Ocean Modell.*, 300–326, doi:10.1016/j.ocemod.2007.02.005.
- Zhai, X., R. J. Greatbatch, and C. Eden (2007), Spreading of near-inertial energy in a 1/12° model of the North Atlantic Ocean, *Geophys. Res. Lett.*, 34, L10609, doi:10.1029/2007GL029895.

M. Inoue and L. J. Rouse Jr., Department of Oceanography and Coastal Sciences, Louisiana State University, Baton Rouge, LA 70803, USA.

R. Lai, Minerals Management Service, MS 4041, 381 Elden Street, Herndon, VA 20170–4817, USA.

X.-H. Lin and L.-Y. Oey, Program in Atmospheric and Oceanic Sciences, Princeton University, Princeton, NJ 08544, USA. (lyo@princeton.edu)

S. E. Welsh, Coastal Studies Institute, Louisiana State University, Baton Rouge, LA 70803, USA.